Application of dynamic speckle methods to study thermal denaturation of the albumin

Xinzhong Li[1*], Yuping Tai[2], Zhaogang Nie[3], Qingdong Chen[1], Liben Li[1]

[1]School of Physics and Engineering, Henan University of Science and Technology,
 Luoyang, 471003, P.R. China

[2]School of Chemical Engineering and Pharmaceutics, Henan University of Science and Technology,
 Luoyang, 471003, P.R. China

[3]College Department of Applied Physics and Chemistry and Institute for Laser Science,
 University of Electro-Communications, Tokyo 182-8585, Japan

*Corresponding author: lixinzhong7922@163.com

The process of the thermal denaturation of albumin was studied using dynamic speckle methods, which included the time history of speckle patterns (THSP), the THSP based on wavelet entropy (WE), speckle size measurement and the speckle pattern mean contrast techniques. In experiments, the dynamic speckle pattern sequences produced from the albumin colloid during heat denaturation were obtained using CCD camera. And then, using these dynamic speckle methods, the change of the movement properties of protein particles was analyzed during the heating process. All results show that the protein particles become bigger, their mean free path becomes shorter and the velocity of the Brownian movement becomes slower during the heating process. The experiments prove that dynamic speckle methods are useful tools to investigate the particles motion in solution.

Keywords: dynamic speckle, albumin, thermal denaturation, protein particles.

1. Introduction

Protein is a long chain molecule linked by twenty kinds of alpha-amino acids, and it is one kind of important biopolymer, which has been used in bioscience, pharmacy, food, feed and clinical examination, and so on. Albumin is one crucial kind of protein, which can be divided into ovalbumin, lactalbumin, seralbumin, *etc*. The protein molecules are easily affected by external factors such as temperature and denaturant, which results in structural change and lost bioactivity, this process is called "protein denaturation" [1]. Denaturation is the modification of the native structure of a protein without cleavage of peptide bonds within the amino acid sequence.

During the past decade, many approaches have been applied to study the properties and functions of albumin, which include optical coherence tomography (OCT) [2],

X-ray scattering [3], electrophoresis [4] and ultrasound [5]. However, among the previously employed methods, there are some disadvantages which limited their applications, including more expensive, poor real-time, invasive, and sampling determination. Therefore, it is important to develop a novel technique to measure the denaturation process of albumin.

Laser speckle is an interference pattern produced by light reflected or scattered from diffusers of the illuminated surface, which is rough compared with the wavelength of the illuminating light. If the scattered particles are moving, a time-varying speckle pattern will be produced at each pixel in the image, which is called "dynamic speckle" or "biospeckle" [6–8]. The spatial and the temporal intensity variations of this pattern contain information of the scattered particles.

Recently, dynamic speckle methods have been used frequently in medical biology measurements [9–13]. Among those applications, there are two major hot points. First one is the time history speckle patterns (THSP) [14, 15] and its gray level co-occurrence matrix (GLCM), for example, assessment of seed viability investigation [10], biospeckle assessment of bruising in fruits [11], particles aggregation monitoring by speckle size measurement and application to blood platelets aggregation [13, 16, 17]. And the other focused on the speckle pattern mean contrast method [18, 19], blood flow monitoring [20, 21] and monitoring the thermal-induced changes in tumor blood flow [22], determining regional heart function [23], and so on.

Dynamic speckle methods have many advantages such as real-time, non-contact, non-invasive, low price, *etc*., which meet the need of determination of the thermal denaturation of the albumin. To our knowledge, there were few reports on studies of the thermal denaturation of albumin using dynamic speckle methods found in published papers though they have been applied popularly in biology.

In our case, the thermal denaturation process was determined real-time and dynamically using dynamic speckle methods, including THSP, THSP based WE, speckle size measurement, and the speckle pattern mean contrast. The movement properties of protein particles in the albumin fluid were studied.

2. Dynamic speckle patterns processing techniques

In this section, we are going to make a short description of different methods employed to process dynamic speckle patterns, including THSP, THSP based on wavelet entropy [24, 25], speckle size measurement [13, 16, 17] and speckle pattern mean contrast [18, 19, 26].

2.1. THSP and THSP based on WE

The time history of speckle patterns (THSP) was proposed to analyze the dynamic speckle patterns generated from active media. If each speckle pattern size is $256{\times}256$ pixel, a new image is composed by setting side by side, the chosen column of the first image, the same column of the second image, the same column of the third image, and so on, 256 times. As a result, a new $256{\times}256$ pixel composite image is then

constructed, namely, the THSP. Its rows represent different points on the object and the columns their intensity state in every sampled instant.

When a phenomenon shows low activity, time variations of the speckle pattern are slow and the THSP shows a horizontally elongated shape. Conversely, when the phenomenon is very active, the THSP shows fast intensity variations that resembled an ordinary spatial speckle pattern.

The THSP images could be analyzed using the inertia moment (IM) of the gray level co-occurrence matrix (GLCM), which is defined as

$$P(i, j) = [N_{ij}] \tag{1}$$

The entries are the number N of occurrences of a certain intensity value i that is immediately followed by an intensity value j. In the spatial case, its principal diagonal is related to homogeneous regions and the nonzero elements far from it represent high contrast occurrences. As the sample shows activity intensity values change in time and the number N outside the diagonal increases and the matrix resembles a cloud. Nevertheless, this matrix is sparse; it is mostly composed by zero values.

For normalization purposes, it is convenient to divide each row of this matrix by the number of times that the first gray level appeared. There are $2(N-1)$ points horizontally adjacent in each row of the GLCM, and by multiplying them by the number of rows N we obtain the total number of the adjacent points of $2N(N-1)$ in the GLCM. Finally, the normalized matrix of GLCM can be written as,

$$p_{ij} = \frac{P(i, j)}{2N(N-1)} \tag{2}$$

Then, using the inertia moment (IM) of the matrix with respect to that diagonal in the row direction, the spread of the GLCM is measured, and the calculated equation is given as,

$$\text{IM} = \sum_i \sum_j (i-j)^2 p_{ij} \tag{3}$$

The occurrences in the diagonal do not contribute to increases in the IM-value while far away P entries add their more heavily weighted values.

Wavelet transform has been proposed in many areas as a tool to deal with signals, without loss of any information, one which enables the analysis of the signal locally as well as globally by dilation and translation of wavelet function. The wavelet analysis method analyzes a signal by means of an amplitude distribution in an appropriate wavelet basis.

Using entropy as a summary, the wavelet transform (WT) has been employed to analyze the dynamic speckle patterns. The process of using wavelet entropy to analysis the THSP is as follows: firstly, the THSP rows are divided into equal temporal windows of number of N. And then, each window is decomposed by multi-level using wavelet family; furthermore, the mean wavelet energy of each detail signal and the total energy

of each temporal window are calculated. Finally, according to the Shannon entropy theory, the wavelet entropy (WE) at each time window of the signal is defined by the following expression.

$$S_{\text{WT}}^{(k)} = -\sum_{l<0} p_l^{(k)} \ln\left[p_l^{(k)}\right] \tag{4}$$

In this expression, every symbol is defined in detail as in reference [27]. According to information theory, entropy is a relative measure of order or disorder in a dynamical system. The more regular the signal, the lower its entropy is. This means that the entropy is inverse proportional to the regular activity. Therefore, while entropy based on the WT indicates the degree of order/disorder of the signal, it can provide additional information about the underlying dynamical process.

2.2. Speckle size measurement

If the media is weak scattering media and the particle size is from 0.53 to 6.36 µm, the speckle sizes of the speckle patterns are proportional to the particle sizes in the media [13]. The speckle size measurement method was proposed by PIEDERRIÈRE *et al.* [13, 16, 17], which calculated the normalized autocovariance function of the intensity speckle pattern obtained in the observation plane (x, y). This function has a zero base and its width provides a reasonable measurement of the "average width" of a speckle. The normalized autocovariance function of the intensity is given by Eq. (5),

$$c_l = \frac{R_I(x, y) - \langle I(x, y)\rangle^2}{\langle I(x, y)^2\rangle - \langle I(x, y)\rangle^2} \tag{5}$$

with $R_I(x, y) = \text{FT}^{-1}[\text{PSD}_I(\nu_x, \nu_y)]$, the PSD is the abbreviation of the power spectral density. $\langle\ldots\rangle$ corresponds to a spatial average.

According to the Wiener–Khintchin theorem, the autocorrelation function of the intensity is given by the inverse Fourier transform of the power spectral density (PSD) of the intensity,

$$\text{PSD}_I(\nu_x, \nu_y) = \left|\text{FT}[I(x, y)]\right|^2 \tag{6}$$

where FT is the Fourier transform.

Substituting Eq. (6) into Eq. (5), the speckle size can be calculated from the following equation,

$$c_l = \frac{\text{FT}^{-1}\left\{\left|\text{FT}\left[I(x, y)\right]\right|^2\right\} - \langle I(x, y)\rangle^2}{\langle I(x, y)^2\rangle - \langle I(x, y)\rangle^2} \tag{7}$$

The horizontal average speckle size dx and the vertical average speckle size dy are calculated from the equations of $C_I(\mathrm{d}x/2, 0) = 0.5$ and $C_I(\mathrm{d}y/2, 0) = 0.5$, respectively.

2.3. Speckle pattern mean contrast

In the case of weak scattering media, the particle sizes are usually less than the illuminating wavelength. When laser beam illuminates the weak scattering media, the central limit theorem is no longer satisfied in the back speckle scattering field. We will get the non-Gaussian statistics of complex speckle amplitudes, which was a partially developed speckle.

For non-Gaussian speckle field speckle contrast is weaker for small particles than for big ones. Speckle contrast K is defined as the ratio of the standard deviation σ_s and the mean local spatial speckle intensity fluctuations $\langle I \rangle$

$$K = \frac{\sigma_s}{\langle I \rangle} \tag{8}$$

The contrast in a speckle image produced by coherent light provides information about the internal particles of the medium being studied [28].

3. Experiments

Figure 1 illustrates the experimental set-up. The He-Ne laser with 10 mW at 632 nm emitted a 1.5 mm-wide beam and its coherent length was about 25 cm. In experiments, the cuvette was made full with a sample of bovine serum albumin (BSA) (Sigma Chemical Co., St. Louis, Mo.) The sample was a weak scattering medium and the particle original size was 0.6 µm. In our case, the heating temperature range was within 30–80 °C and the heating rate was 5 ° per minute. In order to avoid the light beam scattering from the cuvette directly illuminating the imaging array of CCD camera and leading to excessive exposure, the CCD camera was placed apart from the optical axis at an angle of $\theta = 5\ °C$ and the distance D between the cuvette and the CCD camera was 50 cm, as the speckles on the CCD image array must be large as compared to the pixel size and their amount must be sufficient for resolving variations in speckle intensity and ensuring the meaningful statistical evaluation, at the same time.
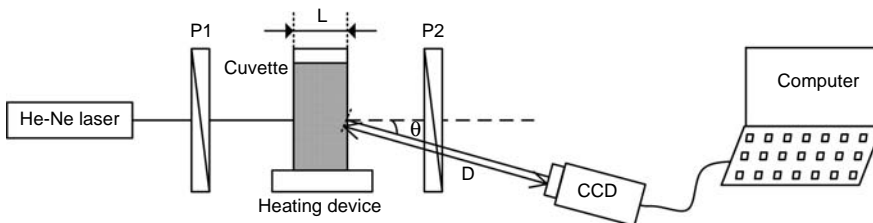

Fig. 1. Experimental set-up of speckle interference.

A polarizer (P1) was placed in the beam before the cuvette ensuring that incident coherent light was linearly polarized. The second polarizer (P2), was placed before the CCD camera, having the same polarization direction as the first one, ensuring that the image plane was not illuminated with differently polarized light that would blur the image and therefore reduced the coherent effects [29]. The speckle sequences were captured at a speed of 25 fps and the size of each speckle pattern was 256×256 pixel, which were stored into the personal computer for processing. Because the sample was a weak scattering medium, the images were non-Gaussian speckle patterns.

After that, in order to verify the dynamic speckle methods, we used differential scanning calorimetry (Diamond DSC) to measure the thermal characteristics of the same albumin sample. Aliquots of the albumin solution were placed in preweighed DSC pans and the pans were hermetically sealed and weighed accurately. The samples were placed in the PerkinElmer Pyris 6 DSC and scanned from 30 to 100 °C at a programmed heating rate of 5 °C/min. The DSC was calibrated by use of indium standards. For each run, an empty sample pan was used for reference. The heat of transition (DH) and peak temperature of denaturation (Td) were computed from the thermal curve. DH values were given as corrected per unit weight of albumin. All DSC measurements were done in duplicate at least.

4. Results and discussion

In our case, the dynamic speckle patterns were obtained and their middle columns were extracted to make THSP images. And then, using wavelet entropy method, the movements of protein particles were analyzed from the THSP images.
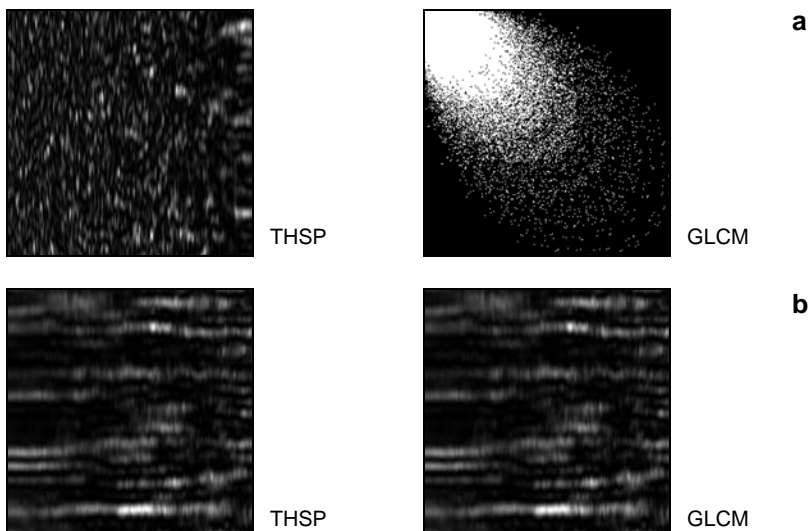

Fig. 2. The THSP image and its GLCM obtained in former heating process (**a**) and latter heating process (**b**).

Figure 2 shows two THSP images and its GLCM images at former heating stage (Fig. 2**a**) and latter heating stage (Fig. 2**b**). From Fig. 2 we can clearly see that at the former heating stage the THSP image was filled with speckles and only on its right margin there appeared some fringes, which means that the corresponding speckle pattern sequence changes fast. So, the Brownian movement of protein particles became fast in the initial heating process. Conversely, in the latter heating stage, the aggregation of protein particles becomes intense and the particles become larger, which made the Brownian motion slow, the mean free path and the velocity of the particles become small, which can be seen from Fig. 2**b**.

Using db4 wavelet family, their 128 rows of the THSP of Figs. 2**a** and 2**b** were processed by wavelet transform, whose intensity fluctuations and their fifth level wavelet decomposition and time evolution images are shown in Figures 3 and 4,
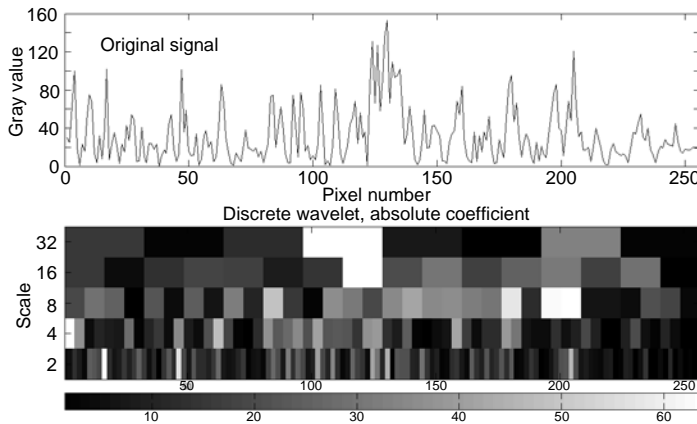
Fig. 3. The speckle signal evolution and its discrete wavelet transform (DWT) decomposition at the 128th row of the THSP image of Fig. 2**a**.
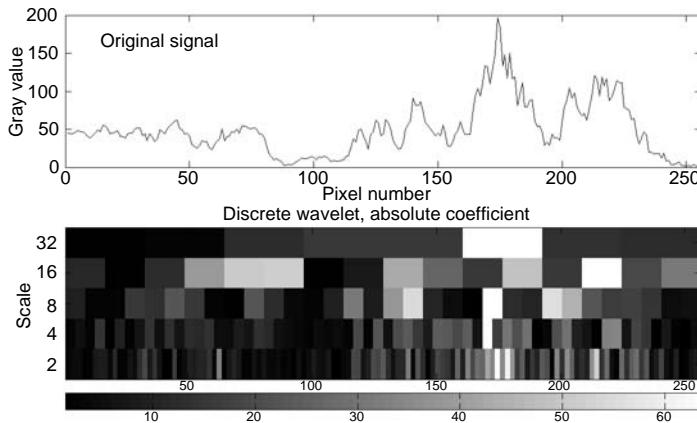
Fig. 4. The speckle signal evolution and its discrete wavelet transform (DWT) decomposition at the 128th row of the THSP image of Fig. 2**b**.

respectively. By comparing these two figures, we can see that the intensity fluctuation of the former heating stage was larger than the latter heating stage which means that the motion of the protein particles became gradually slower.

And then, we analyzed one of the THSP images during the heating process using wavelet entropy. Each row of this THSP was divided into 8 non-overlapping time windows with 32 samples each (the image row includes 256 pixels). Using the db4 orthogonal wavelet family, a three level decomposition was accomplished on each segment. So, the wavelet entropy of each time window was achieved by Eq. (4). Figure 5 shows the wavelet entropy values of eight windows in the middle row of this THSP, which indicates that the entropy values monotonically decreased from 0.82 to 0.35. Correspondingly, the movement of protein particles changed from irregular to regular, which was in agreement with the above analysis.
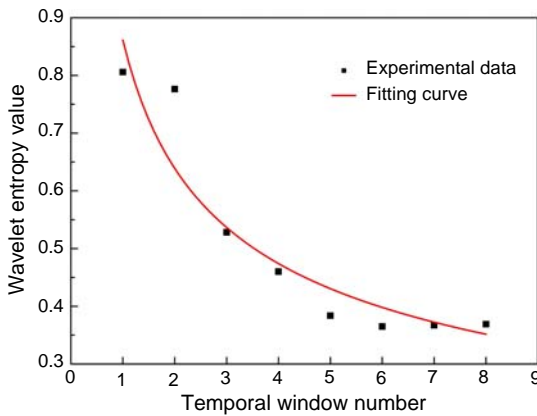

Fig. 5. Wavelet entropy values of different temporal windows.

For visualizing the changing process of WE values of dynamic speckle patterns, the wavelet entropy plots were encoded in gray scale. The process was as follows: firstly, 256 THSP images were generated by extracting the same row from the 1st to the 256th of the 256 dynamic speckle patterns. Then, each row of each THSP image was divided into eight equal size windows and their wavelet entropy was calculated, which resulted in a WE matrix of 256×8. When all of the 256 THSP images were processed, we got a three-dimensional WE matrix of 256×256×8, which could be seen as eight two-dimensional WE matrixes of 256 256. Finally, these eight WE matrixes were made into 256 gray level images, which are shown in Fig. 6.

Figure 6 is composed of eight WE images, which for distinction purposes are cut by white lines and arranged by the following matrix

$$\begin{pmatrix} I_1 & I_2 & I_3 & I_4 \\ I_8 & I_7 & I_6 & I_5 \end{pmatrix}$$

In Figure 6, the dark color represents lower WE values, the bright region means higher WE values.
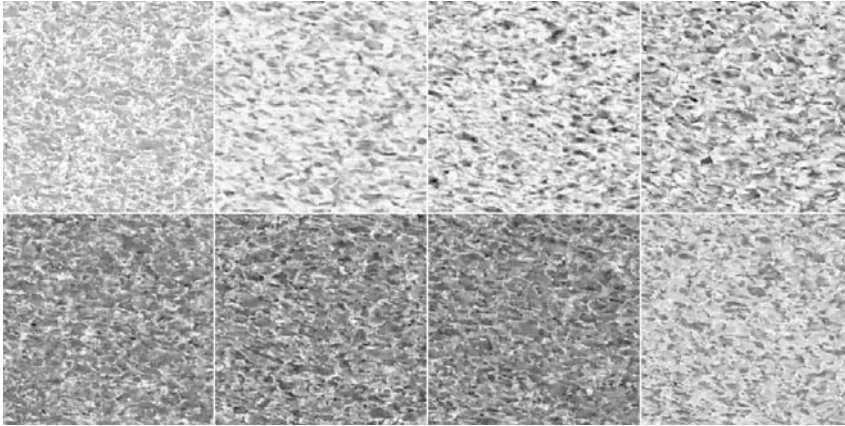
Fig. 6. The wavelet entropy images at different time windows.

From Figure 6, we can see that the change of this 256 speckle pattern sequence was divided into two stages: the stage of $I_1 \sim I_5$ and the stage of $I_6 \sim I_8$. In the former heating process (corresponding to $I_1 \sim I_5$), the values of WE become bigger gradually, which meant that the Brownian motion of the protein particles was active, and the particles were aggregated and flocculated. Each image was divided into some subsets in which the WE values were the same and there was an apparent border between subsets; we call this "localization characteristics". It was different, in the latter heating process of $I_6 \sim I_8$, where the localization was still apparent but its color became darker, in other words, the WE values decreased drastically, which meant that the signal change of the speckle became more irregular. The probable cause is that the protein particles aggregate locally during the heating, and then, the mean free path becomes shorter, and the movement of the particles becomes slower.

Then, the speckle sizes of dx of the first 1500 speckle patterns were calculated by the approach mentioned in Section 2.2. The results are given in Fig. 7, which shows that the speckle size of dx increased gradually from 60 to 83 µm (the pixel size of our camera is approximately 10 µm) during the heating process with corresponding
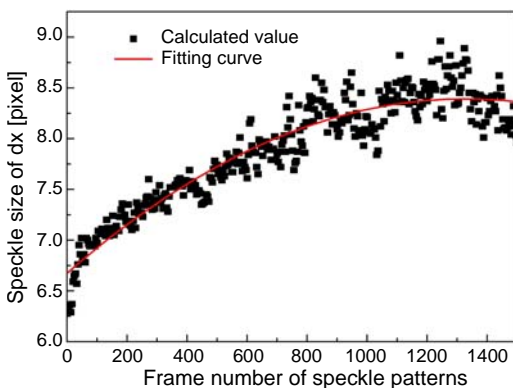

Fig. 7. The speckle size of dx versus the frame number.

the increase of the protein particle size. The phenomenon as the Ref. [13] reported did not find, in which the same speckle size sometimes corresponded two different particle sizes in the solution at a given optical thickness. The probable cause is that the sizes of protein particles were always within 0.53 to 6.36 µm in our case.

And now, using the method presented in Section 2.3, the contrast ratio of four different speckle patterns was calculated locally within a 64×64 pixel subregion, and we then scanned this subregion throughout the whole speckle pattern in 4-pixel increment to form an image of the contrast ratio within the speckle pattern domain. The contrast images are shown in Fig. 8. In these images, red represents a higher contrast ratio and blue represents a lower contrast ratio.

The four contrast images of Fig. 8 are produced from four temporal sequence speckle patterns. Consequently, Figs. 8**a** to 8**d** can represent the heating time. We know that the average contrast value increased from (**a**) to (**d**).The contrast values of these four images increase with the heating time. In previous study [28], the contrast decreases as the number of scatterers increases in weak scattering media. In Fig. 8**a**, one can see a lower contrast ratio, which is consistent with the fact that more scatters result in a lower contrast ratio. Conversely, in Fig. 8**d**, there was a higher contrast ratio localized in the center of the image, which is consistent with the expectation that less scatters result in a higher contrast ratio. The results were in agreement with those of the other methods used above.

At last, the albumin thermal denaturation characteristics were measured by DSC. Figure 9 shows the DSC trace obtained at a heating rate of 5 °C/min. The dominant
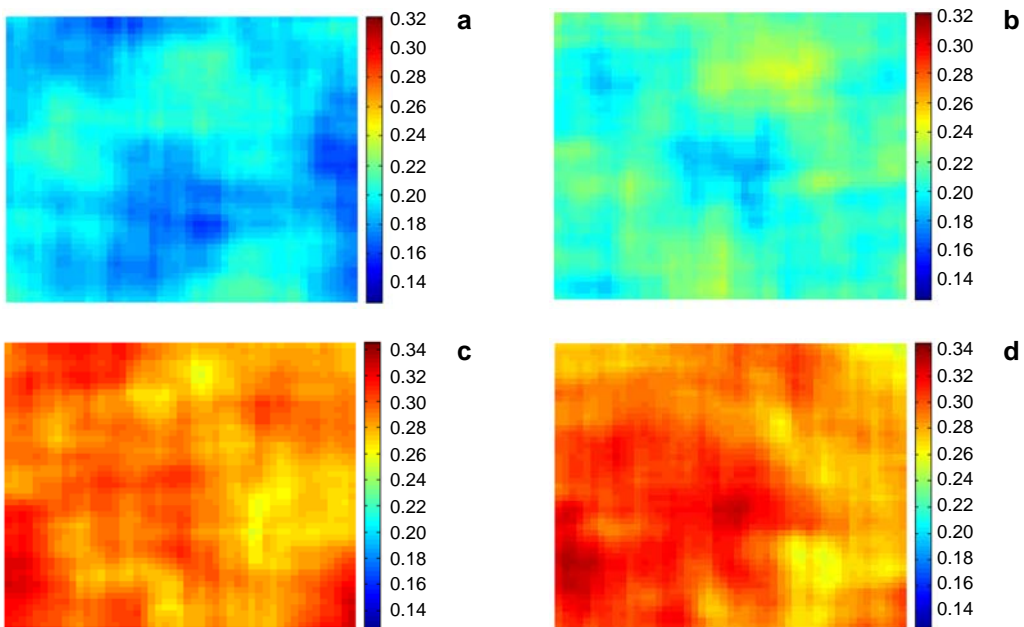

Fig. 8. Speckle contrast of four different stages (see text for explanation).
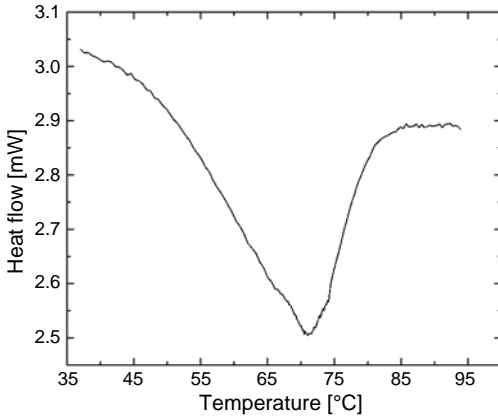
Fig. 9. The DSC curve of albumin denaturation.

endotherm centred at 72°C can be assigned to denaturation of albumin. Denaturation of albumin has a gradual course, which causes gelation and then sedimentation, which means that the dynamic speckle approach is effective. The albumin denaturation can be explained qualitatively using dynamic speckle method.

If we want to further study this process quantitatively, the particle scattering theory should be used simultaneously. Notwithstanding its limitation, this study supplies a quick and simple measurement method for monitoring thermal denaturation of albumin.

5. Conclusions

The thermal denaturation process of the albumin was investigated using dynamic speckle methods, including THSP and THSP based on wavelet entropy, speckle size measurement, and the speckle pattern mean contrast measurement techniques. All results show that the aggregation and flocculation of protein particles occurred during the process of heating which resulted in that the particles became bigger and their free mean path became shorter, and then the movement of protein particles became slower.

Our next work will investigate the protein molecular conformation using dynamic speckle methods and the influence of biological functions [30, 31] by the thermal denaturation of the albumin. Moreover, the factors of the protein concentration, ionic strength and pH of the albumin will be considered.

References

[1] GOETZ J., KOEHLER P., *Study of the thermal denaturation of selected proteins of whey and egg by low resolution NMR*, LWT – Food Science and Technology **38**(5), 2005, pp. 501–512.
[2] MCNALLY K.M., SORG B.S., BHAVARAJU N.C., DUCROS M.G., WELCH A.J., DAWES J.M., *Optical and thermal characterization of albumin protein solders*, Applied Optics **38**(31), 1999, pp. 6661–6672.

[3] WIERENGA, P.A., VAN NOREL L., BASHEVA E.S., *Reconsidering the importance of interfacial properties in foam stability*, Colloids and Surfaces A: Physicochemical and Engineering Aspects **344**(1–3), 2009, pp. 72–78.

[4] MATSUDOMI N., TAKAHASHI H., MIYATA T., *Some structural properties of ovalbumin heated at 80 degrees C in the dry state*, Food Research International **34**(2–3), 2001, pp. 229–235.

[5] WARIS B.N., HASAN U., SRIVASTAVA N., *Stabilisation of ovalbumin by maltose*, Thermochimica Acta **375**(1–2), 2001, pp. 1–7.

[6] DACOSTA G., *Analysis of dynamic phenomena by speckle techniques*, Journal of the Optical Society of America **66**(10), 1976, pp. 1085–1086.

[7] CHIANG F.P., LEE C.H., *Dynamic laser speckle interferometry applied to transient flexure problem*, Applied Optics **16**(12), 1977, pp. 3085–3086.

[8] ZHENG B., PLEASS C.M., IH C.S., *Feature information extraction from dynamic biospeckle*, Applied Optics **33**(2), 1994, pp. 231–237.

[9] ANGELSKY O.V., MAKSIMYAK P.P., *Holographic studies of the dynamic and structural characteristics of biological objects*, Optical Engineering **32**(2), 1993, pp. 267–270.

[10] BRAGA R.A., DAL FABBRO I.M., BOREM F.M., RABELO G., ARIZAGA R., RABAL H.J., TRIVI M., *Assessment of seed viability by laser speckle techniques*, Biosystems Engineering **86**(3), 2003, pp. 287–294.

[11] PAJUELO M., BALDWIN G., RABAL H., CAP N., ARIZAGA R., TRIVI M., *Bio-speckle assessment of bruising in fruits*, Optics and Lasers in Engineering **40**(1–2), 2003, pp. 13–24.

[12] ANGELSKY O.V., DEMIANOVSKY G.V., USHENKO A.G., BURKOVETS D.N., USHENKO Y.A., *Wavelet analysis of two-dimensional birefringence images of architectonics in biotissues for diagnosing pathological changes*, Journal of Biomedical Optics **9**(4), 2004, pp. 679–690.

[13] PIEDERRIÈRE Y., CARIOU J., GUERN Y., LE JEUNE B., LE BRUN G., LORTRIAN J., *Scattering through fluids: speckle size measurement and Monte Carlo simulations close to and into the multiple scattering*, Optics Express **12**(1), 2004, pp. 176–188.

[14] HENAO R., RABAL H.J., TAGLIAFERRI A., TORROBA R.D., *Digital display of the temporal evolution of speckle patterns*, Optical Engineering **35**(1), 1996, pp. 63–69.

[15] RABAL H.J., ARIZAGA R.A., CAP N.L., TRIVI M., ROMERO G., ALANIS E., *Transient phenomena analysis using dynamic speckle patterns*, Optical Engineering **35**(1), 1996, pp. 57–62.

[16] PIEDERRIÈRE Y., LE MEUR J., CARIOU J., ABGRALL J., BLOUCH M., *Particle aggregation monitoring by speckle size measurement, application to blood platelets aggregation*, Optics Express **12**(19), 2004, pp. 4596–4601.

[17] PIEDERRIÈRE Y., BOULVERT F., CARIOU J., LE JEUNE B., GUERN Y., LE BRUN G., *Backscattered speckle size as a function of polarization: Influence of particle-size and- concentration*, Optics Express **13**(13), 2005, pp. 5030–5039.

[18] FUJII H., ASAKURA T., *Contrast variation of image speckle intensity under illumination of partially coherent light*, Optics Communications **12**(1), 1974, pp. 32–38.

[19] GOODMAN J.W., *Dependence of image speckle contrast on surface-roughness*, Optics Communications **14**(3), 1975, pp. 324–327.

[20] CHENG H., YAN Y., DUONG T.Q., *Temporal statistical analysis of laser speckleimages and its application to retinal blood-flowimaging*, Optics Express **16**(14), 2008, pp. 10214–10219.

[21] CHENG H., DUONG T.Q., *Simplified laser-speckle-imaging analysis method and its application to retinal blood flow imaging*, Optics Letters **32**(15), 2007, pp. 2188–2190.

[22] ZHU D., LU W., WENG Y., CUI H., LUO Q., *Monitoring thermal-induced changes in tumor blood flow and microvessels with laser speckle contrast imaging*, Applied Optics **46**(10), 2007, pp. 1911–1917.

[23] KELLY D.J., AZELOGLU E.U., KOCHUPURA P.V., SHARMA G.S., GAUDETTE G.R., *Accuracy and reproducibility of a subpixel extended phase correlation method to determine micron level displacements in the heart*, Medical Engineering and Physics **29**(1), 2007, pp. 154–162.

[24] Braga R.A., Horgan G.W., Enes A.M., Miron D., Rabelo G.F., Filho J., *Biological feature isolation by wavelets in biospeckle laser images*, Computers and Electronics in Agriculture **58**(2), 2007, pp. 123–132.

[25] Passoni I., Pra A.D., Rabal H., Trivi M., Arizaga R., *Dynamic speckle processing using wavelets based entropy*, Optics Communications **246**(1–3), 2005, pp. 219–228.

[26] McKinney J.D., Webster M.A., Webb K.J., Weiner A.M., *Characterization and imaging in optically scattering media by use of laser speckle and a variable-coherence source*, Optics Letters **25**(1), 2000, pp. 4–6.

[27] Blanco S., Figliola A., Quiroga R.Q., Rosso O.A., Serrano E., *Time-frequency analysis of electroencephalogram series. III. Wavelet packets and information cost function*, Physical Review E **57**(1), 1998, pp. 932–940.

[28] Ayers M.R., Hunt A.J., *Observation of the aggregation behavior of silica sols using laser speckle contrast measurements*, Journal of Non-Crystalline Solids **290**(2-3), 2001, pp. 122–128.

[29] Chicea D., *Coherent light scattering on nanofluids: Computer simulation results*, Applied Optics **47**(10), 2008, pp. 1434–1442.

[30] Guerin-Dubiard C., Pasco M., Hietanen A., del Bosque A.Q., Nau F., Croguennec T., *Hen egg white fractionation by ion-exchange chromatography*, Journal of Chromatography A **1090**(1–2), 2005, pp. 58–67.

[31] Huntington J.A., Stein P.E., *Structure and properties of ovalbumin*, Journal of Chromatography B **756**(1–2), 2001, pp. 189–198.